

Optical design of split-beam photonic crystal nanocavities

Aaron C. Hryciw^{1,*} and Paul E. Barclay^(1,2)

¹National Institute for Nanotechnology, 11421 Saskatchewan Drive, Edmonton, Alberta, Canada, T6G 2M9

²Institute for Quantum Information Science, University of Calgary, 2500 University Drive NW, Calgary, Alberta, Canada, T2N 1N4

*Corresponding author: Aaron.Hryciw@nrc-cnrc.gc.ca

Compiled November 6, 2018

We design high quality factor photonic crystal nanobeam cavities formed by two mechanically isolated cantilevers. These “split-beam” cavities have a physical gap at the center, allowing mechanical excitations of one or both of the cavity halves. They are designed by analyzing the optical band structures and mode profiles of waveguides perforated by elliptical holes and rectangular gaps, and are predicted to support optical resonances with quality factors exceeding 10^6 at wavelengths of $\sim 1.6 \mu\text{m}$.

Photonic crystal (PC) nanobeam cavities [1] are currently the subject of intense research interest, as they possess a suite of attractive characteristics: high optical quality factor (Q), wavelength-scale effective mode volume (V_{eff}), low effective mass, and small physical footprint. Integrated within planar photonic waveguide circuitry, PC nanobeam cavities provide an ideal architecture for sensing via cavity optomechanics [2–4]. Many sensing applications are poised to benefit from orders-of-magnitude improvements in sensitivity enabled by on-chip cavity optomechanics, including measurement of mechanical resonators [5], inertial sensing [6], novel platforms for chip-based AFM [7], and detection of torsional motion for magnetometry [8,9]. To maximize the sensitivity of these measurements, devices whose central cavity region is not rigid [10], and can be easily deformed by external forces [?,2,7] are desirable. To this end, here we describe the optical design of a PC nanobeam cavity containing a complete cut through the cavity center, yielding an optical cavity formed by two mechanically uncoupled nano-cantilevers. We show that by careful consideration of the anomalous ordering of the instantaneous band-edge modes at the center of the cavity, a high- Q cavity can be realized in this disconnected structure.

We begin with the deterministic cavity design approach of Quan *et al.* [11,12], the essence of which is to taper the unit cell geometry of a host PC waveguide to effect a linear change in the mirror strength γ , yielding an approximately Gaussian cavity field envelope. Near the band edge of a PC waveguide, the wavevector may be approximated by $k_x = (1 + i\gamma)\frac{\pi}{a}$, with

$$\gamma = \left[\left(\frac{\omega_2 - \omega_1}{\omega_2 + \omega_1} \right)^2 - \left(\frac{\omega_{\text{res}} - \omega_0}{\omega_0} \right)^2 \right]^{\frac{1}{2}} \quad (1)$$

where ω_1 and ω_2 are the lower and upper (respectively) band-edge frequencies defining the optical bandgap of a periodic waveguide, ω_0 is the mid-gap frequency, and ω_{res} is the cavity resonance frequency [12]. A high- Q cavity may be achieved by choosing a host waveguide such that γ at the cavity center is maximized for ω_{res} (minimizing power leakage into the waveguide), and tapering

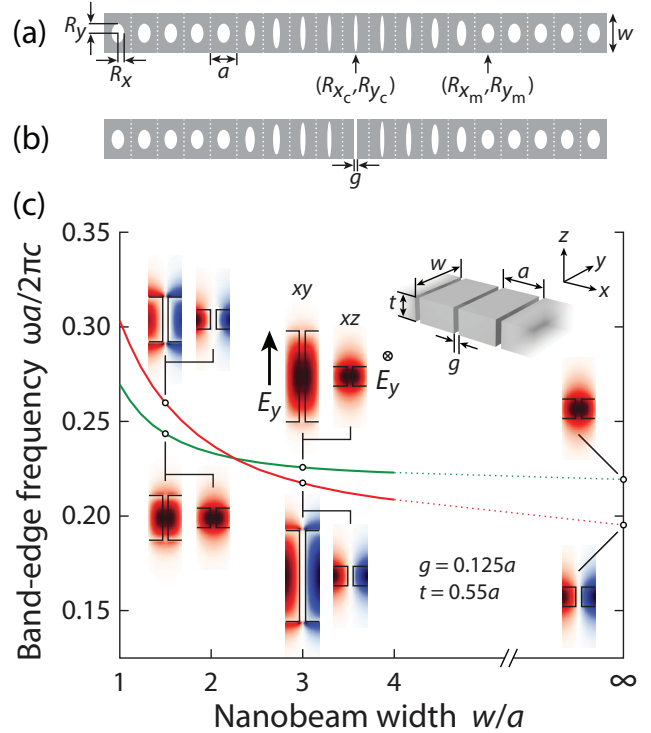


Fig. 1. (a) Donor-mode PC nanobeam cavity with elliptical holes. (b) “Split-beam” PC cavity with a central rectangular gap. (c) “Gap unit cell” band-edge frequencies and electric field profiles for TE-like (y -odd, z -even) modes vs. nanobeam width.

γ away from the cavity center sufficiently adiabatically to limit scattering into radiation modes. A generalized donor-mode cavity (field concentrated in the air holes) with elliptical holes is shown in Figure 1a, tapering from the central hole (R_{x_c}, R_{y_c}) to the “mirror” (host waveguide) hole (R_{x_m}, R_{y_m}) over six segments.

A plausible (albeit naïve) program to construct a PC nanobeam cavity with a central gap is to start with a high- Q design as explained above and simply cut the nanobeam at the cavity center, yielding a “split-beam” cavity capable of supporting a variety of mechanical modes (e.g., axial, torsional, in- and out-of-plane). The

mechanical properties could then be tuned by adjusting the nanobeam supporting structure [?]. A donor-mode cavity, whose field is concentrated in the air regions, allows a strong field overlap with the central gap, whose width may be modulated by mechanical excitations. Intuition suggests that to limit out-of-plane scattering, the central hole unit cell be replaced with a gap unit cell whose band-edge frequency and spatial field profile closely match those of the hole.

To evaluate this design quantitatively, we begin by analyzing a PC waveguide composed of a periodic array of “gap unit cells” formed by dielectric blocks with lattice constant a (along \hat{x}) and thickness t , separated by gaps of width g (centered at $x = 0$). Figure 1c shows the band-edge frequencies and field profiles (E_y) for the lowest-frequency TE-like (y -odd, z -even) modes as the block width w varies, calculated using a 3D frequency-domain eigensolver [13] with a spatial discretization of 32 per period a . A relative permittivity of $\epsilon = 12.11$ (e.g., silicon at a wavelength of 1550 nm) is used throughout.

The crossing in Fig. 1c of the gap PC waveguide band edges reveals an important property of this structure which must be understood to design a high- Q nanobeam cavity with a central gap. In the 2D limit ($w/a \rightarrow \infty$), the ordering of the band-edge frequencies may be explained following the analysis of 1D PCs [14]: the field of the lowest-frequency TE band edge (red line) is concentrated in the dielectric, yielding a higher effective index than the second TE band edge (green line), in which the field is concentrated in the air gap. As w/a changes, the dispersion of the “dielectric” mode is larger than that of the “air” mode, causing the frequency of these modes to cross. Unlike in a 1D PC, for $w/a < 2.25$, the lowest-frequency TE band edge of a gap PC waveguide is an air mode. This crossing behavior is not exhibited in PC nanobeam waveguides with a hole in place of the gap for the considered range of w/a . The difference in dispersion responsible for the crossing can be understood from perturbation theory of moving boundaries [15]: as w changes, the dielectric band edge is shifted more quickly than the air band edge because the dielectric band-edge field overlaps more strongly with the moving waveguide boundary. In contrast, the air band-edge field is concentrated in the gap region, which undergoes no change in shape. This crossing is of crucial importance when designing split-beam cavities, as it governs which of the two gap unit cell band-edge modes should be matched with the band-edge *air mode* (or *dielectric mode* for an acceptor cavity) of the removed central hole.

To illustrate this design paradigm, we investigate three cavities with air-mode resonance wavelengths around 1.6 μm , suitable for fabrication using silicon-on-insulator (SOI) wafers. For a nanobeam with thickness $t = 220$ nm, width $w = 600$ nm, and periodicity $a = 400$ nm, a gap of width $g = 50$ nm corresponds to Fig. 1c with $w/a = 1.5$: the air mode is the lowest-energy TE-like mode. In Fig. 2, we compare the band structure of this rectangular gap unit cell with that of three elliptical

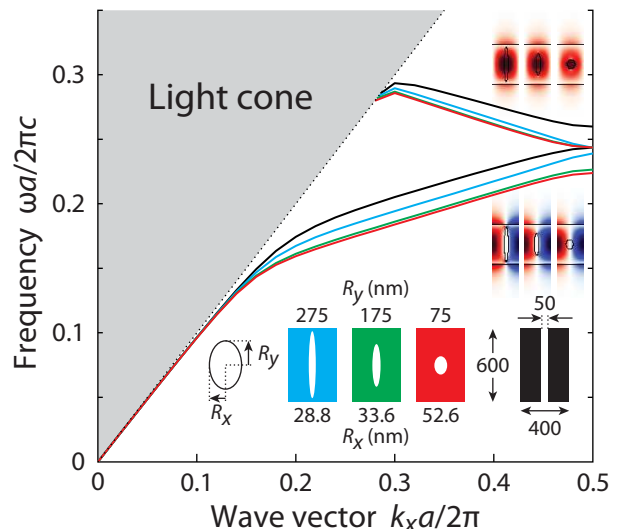


Fig. 2. Band structures of a “gap unit cell” and three elliptical holes unit cells with $\omega_{2\text{ellipse}} = \omega_{1\text{gap}}$. Unit cell geometries are shown in the inset (all units in nm), with $t = 220$ nm. Field profiles of the dielectric (lower) and air (upper) modes for the elliptical holes are shown next to their associated bands.

holes, each satisfying the matching condition that the air-mode band-edge frequencies of the holes and the gap are equal ($\omega_{\text{res}}a/2\pi c = 0.2435$). For y semi-axes of $R_{y_c} = 275, 175,$ and 75 nm, this is satisfied using x semi-axes of $R_{x_c} = 28.8, 33.6,$ and 52.6 nm, respectively.

With two parameters defining their shape— R_{x_c} and R_{y_c} —elliptical holes satisfy the matching condition with a continuum of shapes, plotted with the yellow line in Fig. 3a. The mirror strength γ is calculated as a function of (R_{x_m}, R_{y_m}) using (1); as shown in Fig. 3a, the maximum occurs at $(R_{x_m}, R_{y_m}) = (100, 140)$ nm. To maintain a small nanobeam cavity footprint, we taper the ellipses between the central (R_{x_c}, R_{y_c}) and mirror (R_{x_m}, R_{y_m}) shapes over $N_c = 7$ holes, capping each half-cavity with $N_m = 8$ holes of shape (R_{x_m}, R_{y_m}) . We achieve an approximately linear variation of γ between the central and mirror holes by tapering both semi-axes quadratically: $R_{x_j, y_j} = R_{x_c, y_c} + (j/N_c)^2(R_{x_m, y_m} - R_{x_c, y_c})$, for integer $j \in [-N_c, N_c]$. The hole shapes for the three cavities defined by the central holes in Fig. 2 are plotted as circles in Fig. 3a. The central ($j = 0$) ellipse is then replaced by a 50-nm-wide rectangular gap to complete the design. Note that, up to this point, only band-structure calculations have been used in the design [11].

We assess the performance of these three cavities using finite-difference time-domain (FDTD) simulations [16]; the field profiles for each are shown in Figure 3b, with Q , λ_{res} , and V_{eff} (defined by the peak field strength) listed in the inset to Figure 3a. The overall cavity Q is dominated by scattering perpendicular to the nanobeam, split nearly evenly in the y and z directions; loss into guided modes (x direction) is small due to the large γ of the mir-

ror segments. While all three cavities satisfy the band-edge matching condition described above, significantly less scattering occurs as the fictitious “central ellipse” more closely resembles the cross-section of a rectangular gap (i.e., large R_y), achieving a Q of 3.3×10^6 for the $R_{y_c}=275$ nm cavity. As elucidated in [17], scattering from the band-edge waveguide modes into lossy radiation modes generally increases as the taper between waveguide cross-sections becomes less gradual. In the case of the $R_{y_c}=75$ nm cavity, the poor adiabaticity between the gap and the neighboring hole degrades the Q to 3.6×10^4 .

The band-edge matching condition yields (R_{x_c}, R_{y_c}) values which are very close to optimal for a quadratic taper: a free maximization of Q with respect to R_{x_c} using FDTD yields only a $\sim 20\%$ improvement in Q for the $R_{y_c}=275$ and 175 nm cavities, with a change in R_{x_c} of less than 10%. Alternately, Q may be increased—at the expense of a larger V_{eff} and cavity footprint—by increasing N_c to yield a more adiabatic taper [11]. From an experimental standpoint, Figure 3a illustrates the inherent trade-off in this scheme between Q and practical fabricability: pattern fidelity becomes more difficult for long, narrow elliptical holes due to minimum feature size limits in lithography and etching processes.

By studying the band structure of a nanobeam patterned with an array of gaps, we have demonstrated a technique for designing PC “split-beam” cavities with high Q ($>10^6$) despite the existence of a major perturbation in the cavity region. These cavities support modes whose field is concentrated in the central air gap, and are expected to be well suited for sensing applications involving mechanical actuation of the nanocavity cantilevers. This will be particularly useful for applications such as force sensing and torque magnetometry [9].

We thank M. H. Wu, J. D. Davis, and M. R. Freeman for helpful discussions. This work was supported by NRC, CFI, iCORE/AITF, and NSERC.

References

1. M. Notomi, E. Kuramochi, and H. Taniyama, “Ultra-high-Q Nanocavity with 1D Photonic Gap,” *Opt. Express* **16**, 11 095 (2008).
2. M. Eichenfield, R. Camacho, J. Chan, K. J. Vahala, and O. Painter, “A picogram- and nanometre-scale photonic-crystal optomechanical cavity.” *Nature* **459**, 550–5 (2009).
3. M. Eichenfield, J. Chan, R. M. Camacho, K. J. Vahala, and O. Painter, “Optomechanical crystals,” *Nature* **462**, 78–82 (2009).
4. P. B. Deotare, I. Bulu, I. W. Frank, Q. Quan, Y. Zhang, R. Ilic, and M. Loncar, “All optical reconfiguration of optomechanical filters.” *Nat. Comm.* **3**, 846 (2012). <http://www.ncbi.nlm.nih.gov/pubmed/22617286>
5. E. Gavartin, P. Verlot, and T. Kippenberg, “A hybrid on-chip optomechanical transducer for ultrasensitive force measurements,” *Nat. Nano* **7**, 509514 (2012).
6. A. G. Krause, M. Winger, T. D. Blasius, Q. Lin, and O. Painter, “A high-resolution microchip optomechanical accelerometer,” *Nature Phot.* **6**, 768–772 (2012).

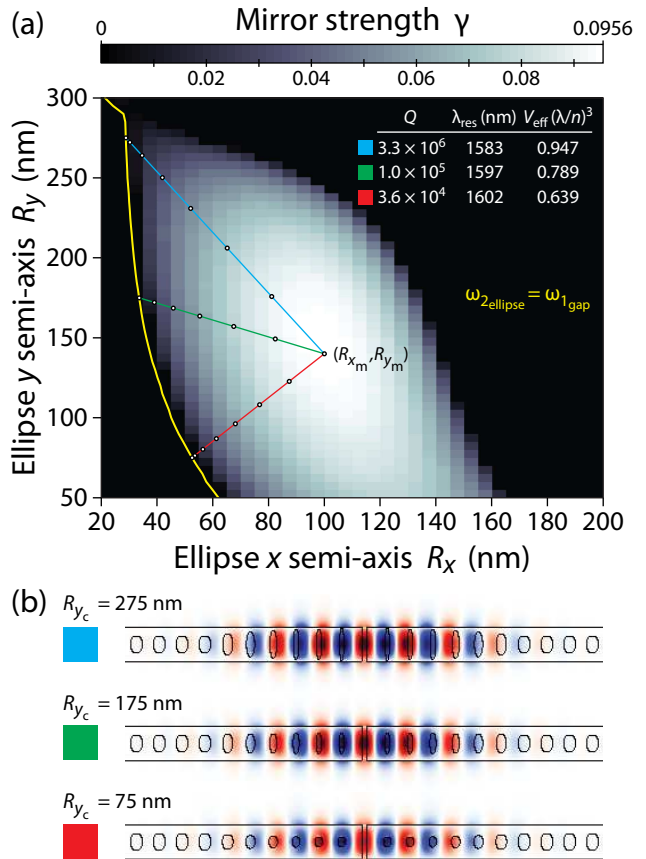


Fig. 3. (a) Mirror strength and design parameters for three split-beam cavities; a , t , and w , and the three (R_{x_c}, R_{y_c}) values are as in Figure 2. The half-cavity tapered ellipse shapes are shown by open circles. (b) Mode profiles (E_y , xy plane) of the three cavities in (a).

7. K. Srinivasan, H. Miao, M. T. Rakher, M. Davanço, and V. Aksyuk, “Optomechanical transduction of an integrated silicon cantilever probe using a microdisk resonator,” *Nano letters* **11**, 791 (2011).
8. J. P. Davis, D. Vick, D. C. Fortin, J. A. J. Burgess, W. K. Hiebert, and M. R. Freeman, “Nanotorsional resonator torque magnetometry,” *Appl. Phys. Lett.* **96**, 72 513 (2010).
9. P. H. Kim, C. Doolin, B. D. Hauer, A. J. R. MacDonald, M. Freeman, P. E. Barclay, and J. P. Davis, “Nanoscale Torsional Optomechanics,” *arXiv preprint arXiv:1210.1852* (2012).
10. M. Li, W. Pernice, and H. Tang, “Broadband all-photonic transduction of nanocantilevers,” *Nature Nano.* **4**, 377–382 (2009).
11. Q. Quan and M. Loncar, “Deterministic design of wavelength scale, ultra-high Q photonic crystal nanobeam cavities,” *Opt. Express* **19**, 18 529–18 542 (2011).
12. Q. Quan, P. Deotare, and M. Loncar, “Photonic crystal nanobeam cavity strongly coupled to the feeding waveguide,” *Appl. Phys. Lett.* **96**, 203 102–203 102 (2010).
13. S. G. Johnson and J. D. Joannopoulos, “Block-iterative frequency-domain methods for Maxwell’s equations in a planewave basis,” *Opt. Express* **8**, 173–190 (2001).

<http://www.opticsexpress.org/abstract.cfm?URI=OPEX-8-3-173>

14. J. Joannopoulos, S. Johnson, J. Winn, and R. Meade, *Photonic Crystals: Molding the Flow of Light* (Princeton University, 2008).
15. S. G. Johnson, M. Ibanescu, M. A. Skorobogatiy, O. Weisberg, J. D. Joannopoulos, and Y. Fink, "Perturbation theory for Maxwell's equations with shifting material boundaries," *Phys. Rev. E* **65**, 66 611 (2002).
16. A. F. Oskooi, D. Roundy, M. Ibanescu, P. Bermel, J. D. Joannopoulos, and S. G. Johnson, "MEEP: A flexible free-software package for electromagnetic simulations by the FDTD method," *Comp. Phys. Comm.* **181**, 687–702 (2010).
<http://www.sciencedirect.com/science/article/B6TJ5-4XRJX96-3/2/97a9289cb9e2b8524b86e1112c1b593b>
17. S. G. Johnson, P. Bienstman, M. A. Skorobogatiy, M. Ibanescu, E. Lidorikis, and J. D. Joannopoulos, "The adiabatic theorem and a continuous coupled-mode theory for efficient taper transitions in photonic crystals," *Phys. Rev. E* **66**, 66 608 (2002).